Cancer Immunology, Immunotherapy (2023) 72:4015–4030
https://doi.org/10.1007/s00262-023-03535-y

RESEARCH

XFab-α4-1BB/CD40L fusion protein activates dendritic cells, improves expansion of antigen-specific T cells, and exhibits antitumour efficacy in multiple solid tumour models

Bochun Wang[1,2] · Yujie Liu[2] · Ruofei Yuan[3] · Xiaoqian Dou[2] · Niliang Qian[2] · Xiujie Pan[2] · Guili Xu[2] · Qinzhi Xu[2] · Bo Dong[2] · Cuima Yang[2] · Hongjie Li[2] · Jingjing Wang[2] · Guijun Bai[2] · Liangfa Liu[1] · Xin Gao[2]

Received: 5 April 2023 / Accepted: 21 August 2023 / Published online: 21 October 2023

Abstract

Background Additional immunotherapies are still warranted for non-responders to checkpoint inhibitors with refractory or relapsing cancers, especially for patients with "cold" tumours lacking significant immune infiltration at treatment onset. We developed XFab-α4-1BB/CD40L, a bispecific antibody targeting 4-1BB and CD40 for dendritic cell activation and priming of tumour-reactive T cells to inhibit tumours.

Methods XFab-α4-1BB/CD40L was developed by engineering an anti-4-1BB Fab arm into a CD40L trimer based on XFab® platform. Characterisation of the bispecific antibody was performed by cell-based reporter assays, maturation of dendritic cell assays, and mixed lymphocyte reactions. The abilities of antigen-specific T-cell expansion and antitumour efficacy were assessed in syngeneic mouse tumour models. Toxicological and pharmacodynamic profiles were investigated in non-human primates.

Results XFab-α4-1BB/CD40L demonstrated independent CD40 agonistic activity and conditional 4-1BB activity mediated by CD40 crosslinking, leading to dendritic cell maturation and T-cell proliferation in vitro. We confirmed the expansion of antigen-specific T cells in the vaccination model and potent tumour regression induced by the bispecific antibody alone or in combination with gemcitabine in vivo, concomitant with improved tumour-reactive T-cell infiltration. XFab-α4-1BB/CD40L showed no signs of liver toxicity at doses up to 51 mg/kg in a repeated-dose regimen in non-human primates.

Conclusions XFab-α4-1BB/CD40L is capable of enhancing antitumour immunity by modulating dendritic cell and T-cell functions via targeting 4-1BB agonism to areas of CD40 expression. The focused, potent, and safe immune response induced by the bispecific antibody supports further clinical investigations for the treatment of solid tumours.

Keywords Cancer immunotherapy · Agonist antibody · CD40 · 4-1BB · Cancer vaccine

Introduction

Recent advances in immunotherapy have revolutionised the paradigm of cancer treatment [1]. Immune checkpoint inhibitors targeting programmed cell death-1 (PD-1), PD-L1, and cytotoxic T-lymphocyte-associated protein 4 (CTLA-4) have gained clinical success for a subset of patients with advanced solid tumours, but additional immunotherapies are still warranted for the substantially unaddressed clinical challenge, particularly for patients with "cold" tumours, which lack significant immune infiltration at treatment onset [2–4]. Addressing deficient T-cell priming and cytotoxicity represents a great opportunity for cancer immunotherapy.

In this context, costimulation of T cells via the tumour necrosis factor receptor superfamily (TNFRSF) member

Bochun Wang, Yujie Liu, and Ruofei Yuan have contributed equally to this work and share first authorship.

✉ Liangfa Liu
liuliangfa301@163.com

✉ Xin Gao
wbcjkl603789@163.com

[1] Department of Otolaryngology Head and Neck Surgery, Beijing Friendship Hospital, Capital Medical University, Beijing 100050, People's Republic of China

[2] Beijing Immunoah Pharma Tech Co., Ltd., Beijing 100141, People's Republic of China

[3] Capital Medical University, Beijing 100069, People's Republic of China

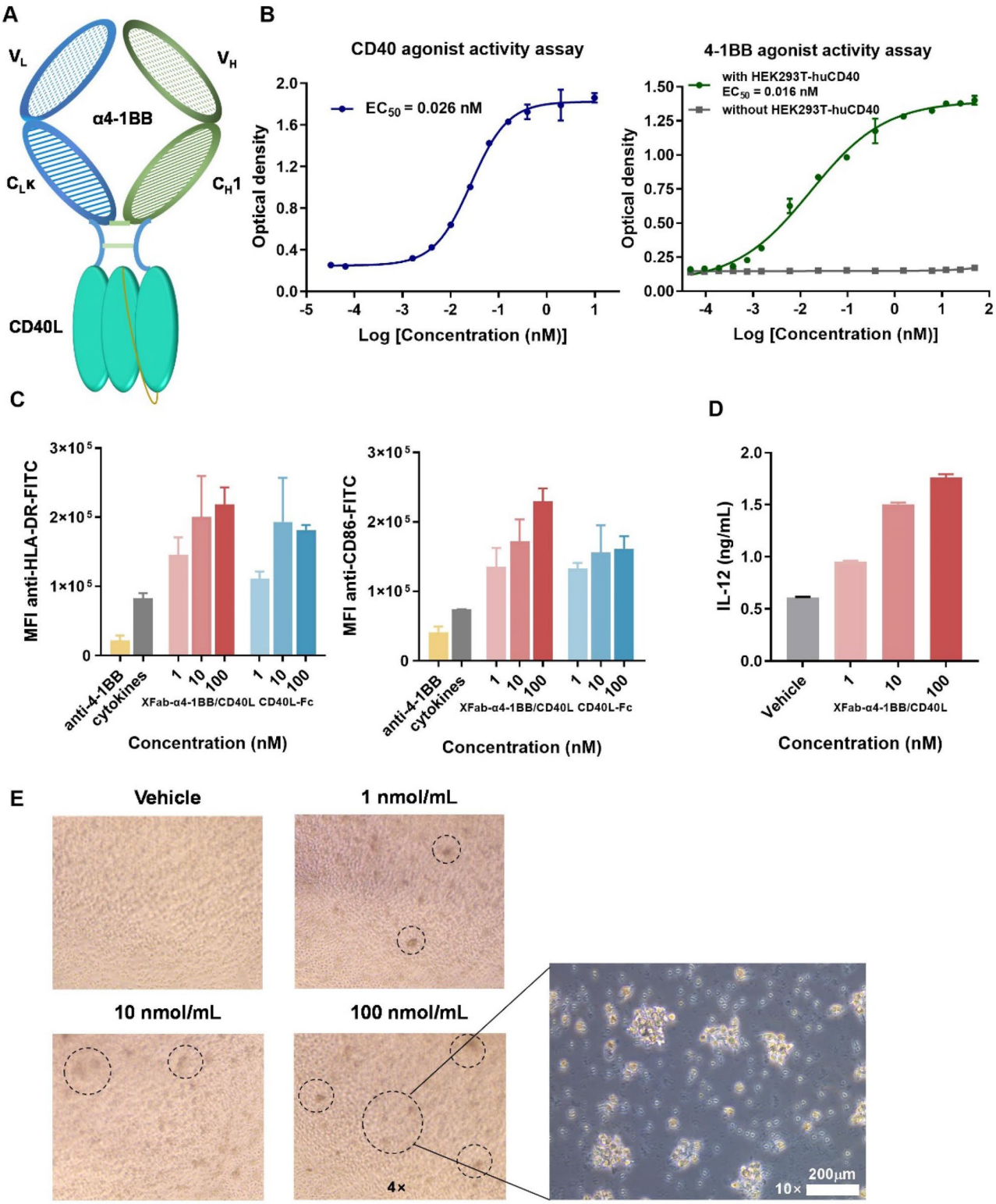

4-1BB (CD137) may represent a promising approach for solid tumours [5]. The costimulatory molecule, 4-1BB, is upregulated on activated T cells [6]. Engagement of 4-1BB provides a survival signal to T cells, thereby enhancing proliferation, cytotoxicity, cytokine production [7–10], and T-cell memory formation [11]. In spite of these preclinical data supporting 4-1BB as a potential cancer immunotherapy target, clinical attempts with agonistic targeted 4-1BB

◂**Fig. 1** The characterisation of XFab-α4-1BB/CD40L fusion protein and maturation of dendritic cell. **a** Schematic representation of the bispecific antibody with a monovalent Fab fragment binding to 4-1BB and a trimetric CD40L binding to CD40. Heterodimerisation and correct assembly are achieved by the interaction between the V_H and V_L domain, and one disulphide bond in the hinge region. **b** XFab-α4-1BB/CD40L displayed independent CD40 agonist activity in HEK-Blue CD40L cells (left). In contrast, the 4-1BB agonist activity was dependent on CD40-expressing HEK293T cells (right). Data shown are mean ± SD of triplicate measurements from one representative results of two independent experiments. **c** DC maturation induced by XFab-α4-1BB/CD40L. Monocyte-derived DCs were incubated with dilution series of XFab-α4-1BB/CD40L fusion protein, CD40L-Fc (100 nM), anti-4-1BB mAb (100 nM), or cytokines (IL-6, IL-1β, and TNF-α) for 48 h. The MFI of CD80 and HLA-DR was detected by flow cytometry. Data shown are the mean MFI ± SD (n = technical duplicates). **d** Supernatant of cultures described in **c** was collected after 48 h and IL-12 secretion was analysed by ELISA. Data shown are mean ± SD of technical duplicates. **e** Phase contrast images were taken after 48 h at 4 × (left) and 10 × (right) magnification. Microcluster formation was observed and highlighted by the dashed circles. Scale bars: 200 µm

monoclonal antibodies (anti-4-1BB mAb), such as urelumab and utomilumab, have demonstrated limited clinical success because of liver safety issues and lack of consistent clinical activity [3]. Unfortunately, the decade-long effort has not pushed agonistic 4-1BB monotherapy beyond early-stage clinical trials.

Several new strategies have emerged to construct agents with multiple specificities and activities including 4-1BB in one molecule [12–18]. Considering the 4-1BB mechanistic rationale and the demand for a better safety profile, the idea of utilising 4-1BB to agonistically cross-link other immune receptors, such as CD40, may be plausible. CD40, a costimulatory receptor belonging to TNFRSF, is expressed on antigen-presenting cells (APC), including dendritic cells (DC), B cells, macrophages, and a variety of non-immune cells including platelets and several types of tumour cells. CD40L, the physiological ligand of CD40, existing on immune cells including T cells, NK cells, B cells, and especially CD4 T cells, can biologically self-assemble into functional trimers which induce CD40 trimerisation and downstream signalling. CD40 serves as a critical role in immunological synapse stimulation, DC maturation, and subsequent activation of antigen-specific T cells. Thus, targeting the CD40 pathway may be pivotal in converting cold tumours to hot ones and further generating effective T-cell immunity. However, single-agent CD40 mAb has yielded minimal rates of objective tumour response in clinic, despite clear evidence of pharmacodynamic activity. Combination therapies will likely be required to unleash the full potential of CD40 targeting.

Inspired by the underlying biology of these two pathways, we anticipate that combining bispecific targeting of 4-1BB and CD40 could awaken the dual function of triggering antitumour immunity. In this study, we describe the generation and preclinical characterisation of the XFab-α4-1BB/CD40L fusion protein (IMB071703), a novel bispecific antibody that exploits the complementary rationales of CD40 activation on DC and 4-1BB crosslinking on T cells. Preclinical proof-of-concept data reveal that the antibody harbour increased potency for DC maturation and T-cell activation, leading to efficient tumour inhibition in multiple tumour-bearing mouse models. In addition, XFab-α4-1BB/CD40L has been shown to serve as an adjuvant and enhance the antitumour efficacy of cancer vaccines as prophylactic treatment.

Results

Design of XFab-α4-1BB/CD40L bispecific antibody

As agonistic anti-4-1BB antibodies have failed in the clinic to date, our goal was to direct potent 4-1BB stimulation to areas of CD40 expression at tumour sites without the need for FcγR crosslinking in a broad range of cancers. We generated the XFab-α4-1BB/CD40L fusion protein (IMB071703), a bispecific antibody characterised by the following features (Fig. 1a): (1) a monovalent Fab fragment binding to 4-1BB and (2) a trimeric split CD40L that binds CD40, considering the natural trimeric form of CD40L in humans. The original Fc region was replaced by a CD40L trimer, leading to 4-1BB receptor clustering and subsequent T-cell activation through CD40-mediated crosslinking.

By biolayer interferometry, XFab-α4-1BB/CD40L bound to human CD40 and 4-1BB with affinities of 26.9 × 10 nM and 16.4 nM, respectively (Supplementary table 1 and supplementary Figure. 1A, B). Binding to both human and cynomolgus cell membrane-associated targets was validated using B cells and 4-1BB-expressing HEK293 T cells (Supplementary Figure. 1C, D).

XFab-α4-1BB/CD40L exhibits independent CD40 and conditional 4-1BB agonist activity

Subsequent investigations aimed to dissect the nature of target crosslinking in receptor activation (Fig. 1b and supplementary Figure. 2). We assessed the CD40 agonist activity using HEK-Blue CD40L reporter cells, which resulted in the secretion of secreted embryonic alkaline phosphatase (SEAP) upon NF–KB activation following CD40 stimulation. In this cell, SEAP secretion was positively correlated with the bispecific antibody concentration. However, in HEK-Blue 4-1BB cells, the downstream signalling and SEAP secretion only occurred in coculture with HEK293T-huCD40 cells, whereas minimal activation occurred in the absence of CD40. These results showed that XFab-α4-1BB/CD40L exhibited independent CD40 agonism, yet

conditional 4-1BB agonist activity dependent on crosslinking to CD40.

XFab-α4-1BB/CD40L induces DC maturation in vitro

To further explore the immunostimulatory effect of XFab-α4-1BB/CD40L at a functional level, we next assayed the bispecific antibody for their ability to mature DCs in vitro. Stimulation of human monocyte-derived DCs with XFab-α4-1BB/CD40L resulted in upregulated expression of the cell surface maturation markers, CD86 and HLA-DR (Fig. 1c), as well as induction of IL-12 (Fig. 1d). Our results demonstrated that the DC maturation was dependent on CD40L arm, as the recombinant CD40L-Fc protein induced similar DC maturation, whereas anti-4-1BB mAb did not. Formation of DC microclusters was also observed in cultures treated with XFab-α4-1BB/CD40L (Fig. 1e). Consistent with the functionality of the CD40 pathway, these data suggested that XFab-α4-1BB/CD40L exhibited potent DC activation in vitro.

XFab-α4-1BB/CD40L enhances T-cell activation and proliferation in vitro

To assess the functionality of XFab-α4-1BB/CD40L furthermore, we addressed immunostimulation of T cells induced by the bispecific antibody in a mixed lymphocyte reaction (MLR) assay. T-cell activation and proliferation was analysed in cocultures of OVA-loaded mature DC with allogeneic T cells in the presence of XFab-α4-1BB/CD40L. The bispecific antibody induced an increase in CD8 and CD4 T-cell proliferation in a dose-dependent manner (Fig. 2a). Upregulation of the activation markers—CD25 (middle) and HLA-DR (late), was observed as well (Fig. 2b). T-cell activation and proliferation induced by XFab-α4-1BB/CD40L were similar to those by anti-4-1BB mAb. The effect of XFab-α4-1BB/CD40L on the interactions between OVA-loaded DCs and T cells was visualised via fluorescence microscopy, where the bispecific antibody preferentially localised to the DC-T-cell surface through target crosslinking (Fig. 2c). Taken together, these findings demonstrated that XFab-α4-1BB/CD40L induced T-cell activation and proliferation through reinforcing the immunological synapse between DC-T-cell surfaces.

XFab-α4-1BB/CD40L results in expansion of antigen-specific T cells in a vaccination model

We used an ovalbumin (OVA) vaccination model to explore how the effect of XFab-α4-1BB/CD40L on DC activation would impact priming of T cells in depth. Briefly, human CD40/4-1BB transgenic mice were immunised with OVA protein and different doses of XFab-α4-1BB/CD40L were injected according to Fig. 3a. We evaluated the potential for antitumour efficacy using OVA as a model cancer vaccine. On day 24, B16-OVA (B16 melanoma cells transfected with OVA) tumours were inoculated, and tumour growth was monitored without any additional treatments following tumour inoculation (Fig. 3b). The results showed that although immunisation with OVA and CD40L-Fc induced slightly delayed tumour growth, this effect was significant enhanced when OVA immunisation was combined with XFab-α4-1BB/CD40L. Fourteen days after the first OVA immunisation, XFab-α4-1BB/CD40L resulted in a markedly detectable expansion of circulating OVA-specific CTL cells, compared to mice receiving OVA only, leading to an increase in the total number of $CD8^+$ effector memory (EM) T cells (Fig. 3c). Although CD40-Fc and anti-4-1BB mAb slightly increased counts of OVA-specific CTL cells and $CD8^+$ EM T cells in tumour tissues at the end point, this change was more prominent with XFab-α4-1BB/CD40L (Fig. 3d). Taken together, these data demonstrate that prophylactic treatment with the bispecific antibody and OVA resulted in improved T-cell activation, expansion of antigen-specific CD8 T cells, and subsequent amplification of memory T-cell pools, leading to OVA-expressing tumour regression.

XFab-α4-1BB/CD40L inhibited tumour growth in syngeneic mouse models

We then examined antitumour efficacy in mouse xenograft model using MC38 cell line. In this model, the bispecific antibody significantly inhibited MC38 cell growth at 50 nmol/kg (Fig. 4a) and a significant dose-dependent survival elongation was observed (Fig. 4b). XFab-α4-1BB/CD40L increased the total number of $CD4^+$ cells, leading to an increased $CD4^+/CD8^+$ ratio (Fig. 4c) in the tumour tissue. This was accompanied by an increased number of effector memory (EM) and central memory (CM) T cells (Fig. 4d). XFab-α4-1BB/CD40L treatment significantly upregulated the expression of 4-1BB and PD-1 on T cells (Fig. 4e), which are two effective markers for tumour-reactive subsets of TILs reported elsewhere [19, 20].

We also evaluated the efficacy of XFab-α4-1BB/CD40L in MB49-bearing male mice, which is considered to have a cold tumour phenotype. Despite the limited efficacy observed in mice treated intravenously, the bispecific antibody exhibited the greatest inhibition of MB49 cell growth at a dose of 15 nmol/kg intratumourally (Fig. 5a, b). Of note, the $CD8/T_{reg}$ ratio significantly increased in this model.

Additionally, mice from our MC38 and MB49 syngeneic tumour studies exhibited no overt signs of toxicity following repeated dosing and maintained normal body weight throughout (Supplementary Figure. 3A, B).

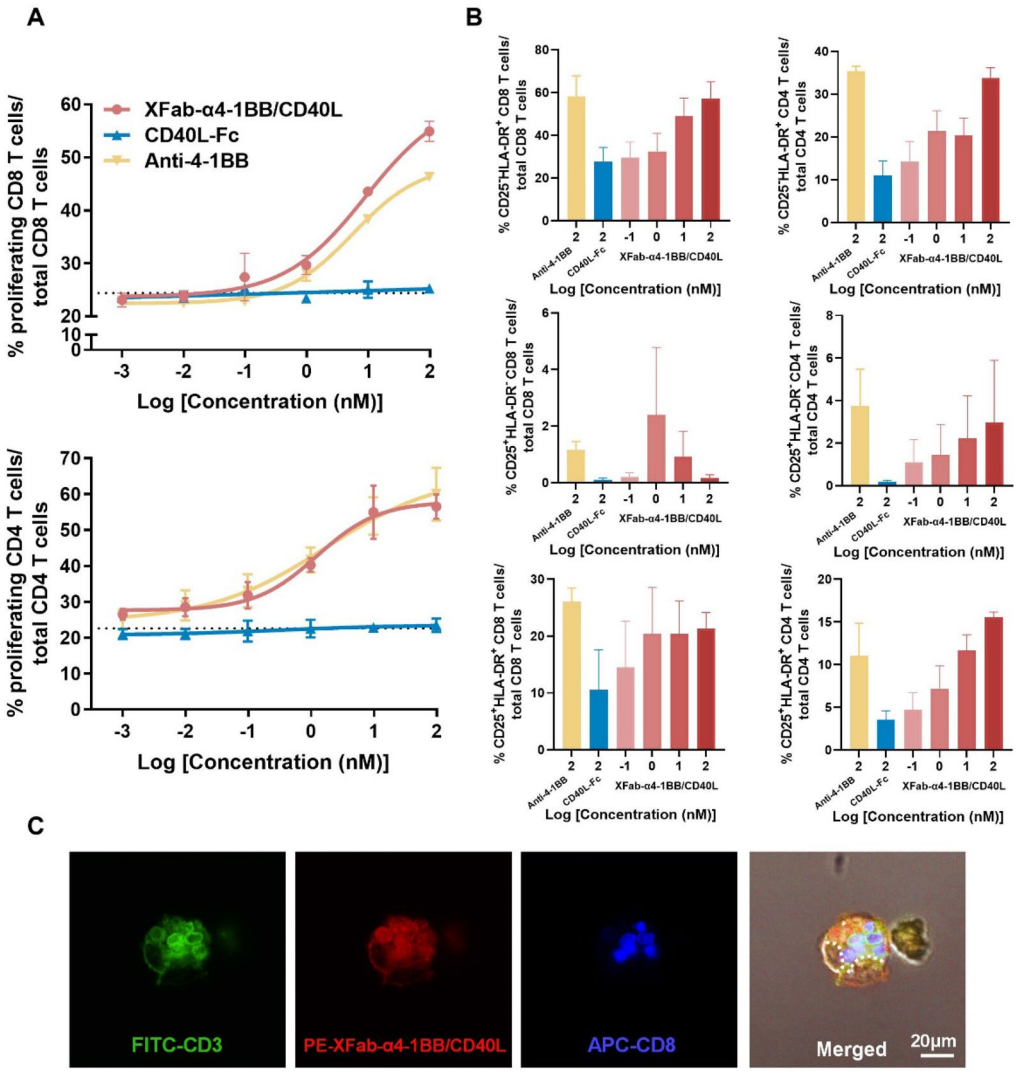

Fig. 2 XFab-α4-1BB/CD40L fusion protein enhances T-cell activation and proliferation in vitro. CellTrace Violet-labelled human T cells were cocultured with ovalbumin–loaded allogenic dendritic cells (DCs) in the presence of titrated bispecific antibody or control antibodies for 10 days. Proliferation (CellTrace Violet dilution) and CD25 and HLA-DR expression of $CD4^+$ or $CD8^+$ cells were analysed by flow cytometry. The percentage of T-cell proliferation (**a**) and the percentage of CD25 and HLA-DR expression (**b**) are shown as mean ± SD (n = technical duplicates). Dotted lines indicate cultures in the absence of treatment. **c** XFab-α4-1BB/CD40L reinforces the immunological synapse through target crosslinking. Representative fluorescent images of DC-T cocultures were used to co-localise FITC-CD3, PE-XFab-α4-1BB/CD40L, and APC-CD8. The white dashed line represents the interface between the DC and T cells. Images were acquired at 40×magnification. Scale bars: 20 μm

Combination of XFab-α4-1BB/CD40L with gemcitabine further enhanced in vivo antitumour efficacy

Pancreatic ductal adenocarcinoma is essentially a cold tumour and responds poorly to immune checkpoint inhibitors. Previous reports have shown that chemotherapy cooperates with immune agonists by spilling antigen [21]. To test the hypothesis that pre-treatment with chemotherapy enhances immune activation, the combination of XFab-α4-1BB/CD40L with gemcitabine was studied in human CD40/4-1BB transgenic mice bearing Panc02 cells. The results showed that either of gemcitabine or XFab-α4-1BB/CD40L induced moderate tumour inhibition, whereas the combination of both agents resulted in enhanced antitumour efficacy (Fig. 6a), accompanied by a significant shift in the T_{reg}/CD4 T cells (Fig. 6b). The upregulation of 4-1BB and PD-1 induced by gemcitabine was further potentiated by combination with XFab-α4-1BB/CD40L (Fig. 6c).

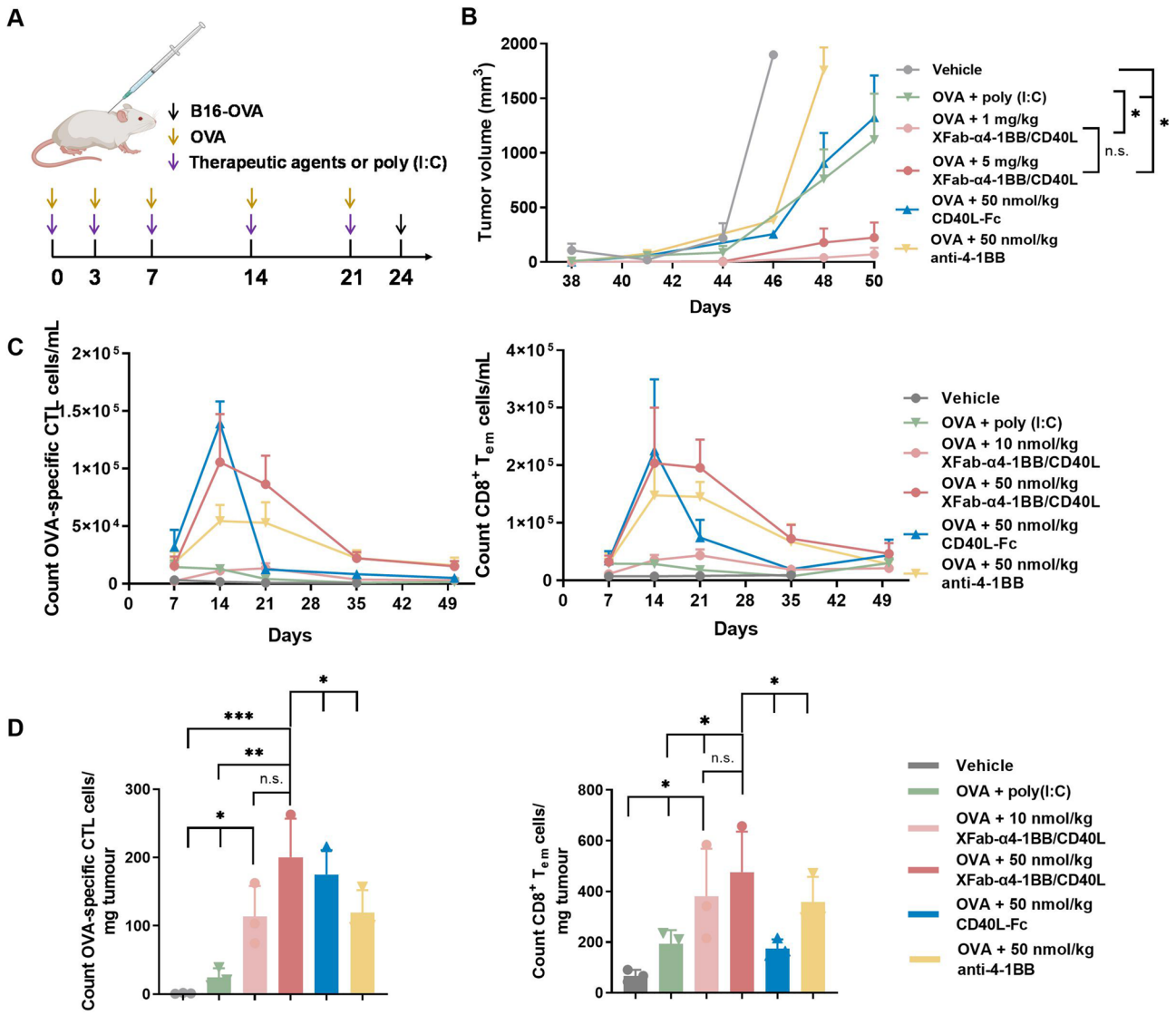

Fig. 3 Repeated dosing of XFab-α4-1BB/CD40L in OVA-rechallenged mice results in expansion of OVA-specific $CD8^+$ cells and inhibited tumour growth in B16-OVA-bearing mice. Human CD40/4-1BB transgenic mice were immunised with 12.5 mg/kg OVA protein and administered indicated dosage of therapeutic agents or 1.25 mg/kg poly (I:C) intradermally on five occasions. On day 24, 5×10^5 B16-OVA cells were inoculated subcutaneously. Whole blood and tumour tissues were collected for flow cytometry. **a** Overview of the experimental set-up. **b** Tumour growth after B16-OVA inoculation. Tumour is displayed until the point where the first mouse in each group approached the ethical tumour volume limit of 2 cm^3 and is sacrificed. **c** Total counts of OVA-specific CTL cells ($CD3^+$ $CD8^+$ $CD44^+$ H-$2K^b$ -OVA tetramer$^+$, left) and total counts of $CD8^+$ effector memory (EM) T cells ($CD3^+$ $CD8^+$ $CD44^+$ $CD62L^-$, right) in blood. **d** Total counts of OVA-specific CTL cells (left) and total counts of $CD8^+$ EM T cells (right) in tumour tissues on day 50. Data points indicate mean ± SEM. $n = 6–7$ per group

Tolerability in non-human primates (NHPs)

Cytokine release syndrome is a dose-limiting complication of T-cell engagers in humans [22]. Although this adverse effect of 4-1BB is perhaps less severe, we sought to explore the potential toxicities of the bispecific antibody via in vitro cytokine release assay by co-incubating human PBMCs with the bispecific antibody. In this assay, no significant difference in cytokine release was observed (Supplementary Figure. 3).

As the binding affinities of the bispecific protein to NHP antigens were validated as shown above (Supplementary Figure. 1C, D), the PK behaviour of XFab-α4-1BB/CD40L was characterised in cynomolgus monkeys following intravenous administration (Supplementary table 2). XFab-α4-1BB/CD40L displayed a dose-dependent increase in C_{max}

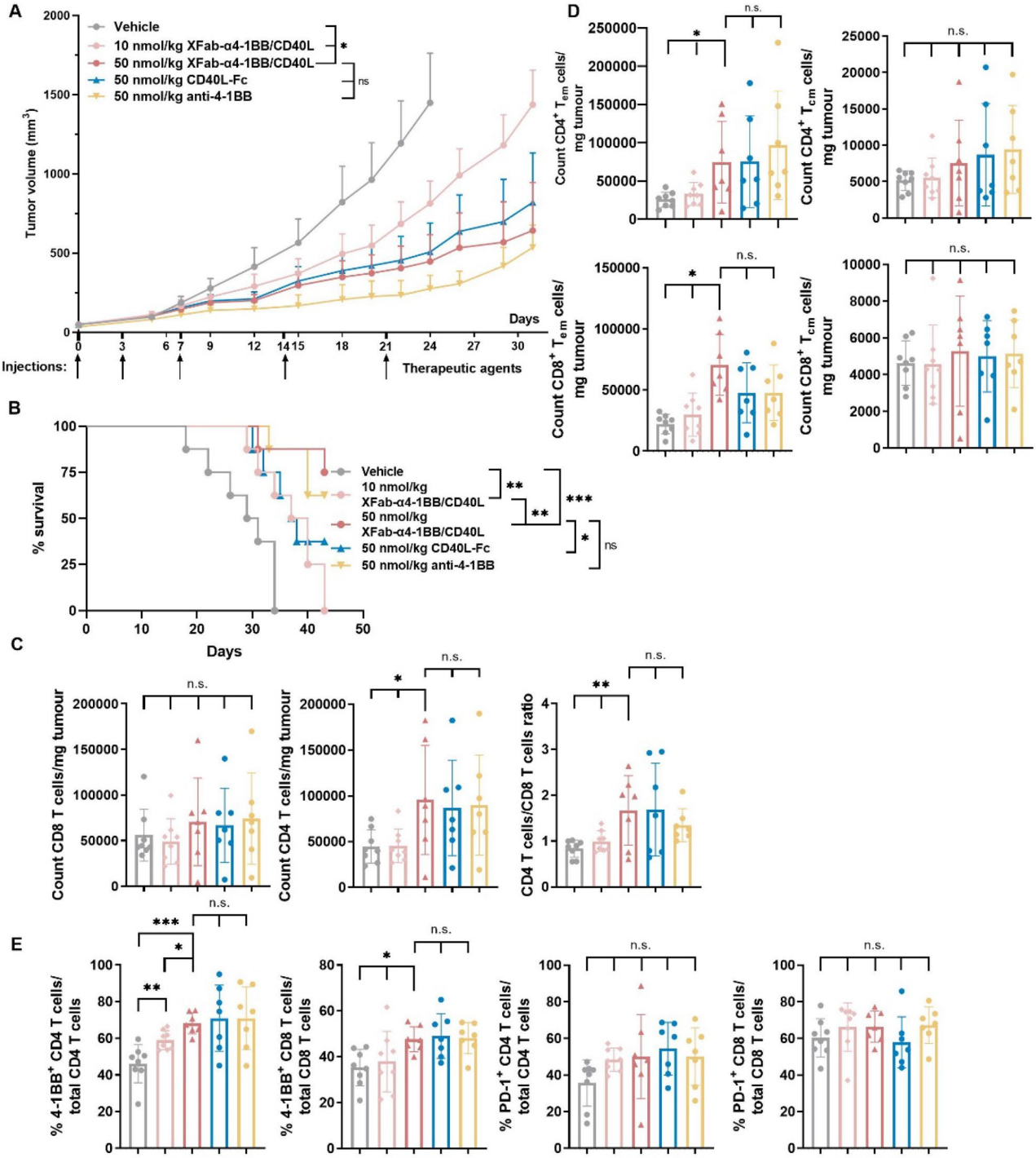

Fig. 4 XFab-α4-1BB/CD40L inhibits tumour growth and increases intratumoural T-cell accumulation and activation in MC38-bearing mice. **a** Randomised human CD40/4-1BB transgenic mice were subcutaneously implanted with MC38 cells at 2.0×10^5 per mouse. When tumours were approximately 50–90 mm^3, the mice were intratumourally administered designated antibodies or vehicle at indicated time points. Tumour burden was quantitated at various time points after treatment. Data points indicate mean ± SEM ($n = 8$ animals per group). Statistical analysis was performed by two-way repeated measure ANOVA with Tukey's multiple comparison test. **b** Kaplan–Meier survival curves of MC38-bearing mice. Statistical significance was analysed by the log-rank test. **c** Digested tumour tissues at the end point were analysed by flow cytometry gating on living $CD4^+$ or $CD8^+$ cells. Shown is mean ± SD. Tumour-infiltrating $CD4^+$ and $CD8^+$ T cells were analysed for memory cell subpopulation (**d**) and 4-1BB and PD-1 expression (**e**) by flow cytometry. Effector memory (EM) and central memory (CM) T cells were defined as $CD44^+CD62L^-$ and $CD44^+CD62L^+$ T cells, respectively. Data points indicate mean ± SD (n = 8 animals per group). Statistical significance in (**c–e**) was calculated using unpaired one-way ANOVA with Tukey's multiple comparison test

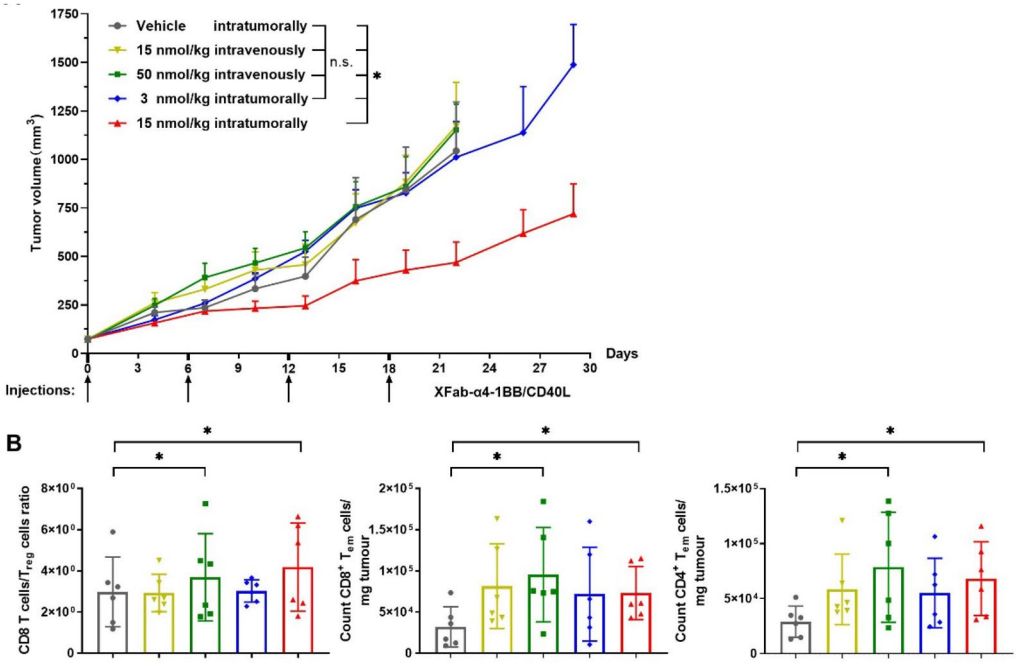

Fig. 5 XFab-α4-1BB/CD40L inhibits tumour growth and increases intratumoural T-cell accumulation and activation in MB49-bearing mice. **a** Randomised human CD40/4-1BB transgenic male mice were subcutaneously implanted with MB49 cells at 2.0×10^5 per mouse. When tumours were approximately 50–90 mm^3, the mice were given intravenous or intratumoural injections of XFab-α4-1BB/CD40L at the indicated time points. Tumour burden was quantitated at various time points after treatment. Data points indicate mean ± SEM ($n = 6$ animals per group). Statistical analysis was performed by two-way repeated measure ANOVA with Tukey's multiple comparison test. **b** Digested tumour tissues at the end point were analysed by flow cytometry gating on subpopulations of T cells. Shown is mean ± SD. Statistical significance was calculated using unpaired one-way ANOVA with Tukey's multiple comparison test

and AUC. The systemic clearance rate (CL) and volume of distribution (Vd) declined as the doses increased. Overall, anti-drug antibodies (ADAs) were detected in 4 (66.7%) of 6 cynomolgus monkeys treated with XFab-α4-1BB/CD40L. There was no evidence to suggest that the pharmacokinetic profiles were altered in monkeys with ADAs.

To further explore potential toxicities of the bispecific antibody, an NHP toxicology study was performed by using a single-dose regimen and a repeated-dose regimen. A single dose of 765 nmol/kg intravenously induced no adverse events in the monkeys (Table 1). For the repeated-dose regimen, animals were necropsied 7 days after the last administration, and liver samples were collected at necropsy for histological assessment. Each liver section was scored for pathology, and the frequencies of monkeys showing zero, minimal, slight, or moderate effects within each group are shown in Table 2. The liver displayed minimal mixed inflammatory cells in periportal tracts, minimal degeneration with mixed inflammatory cells in the parenchyma, and no degenerative hepatocytes. Changes in clinical chemistry parameters related to liver function were also documented (Fig. 7b). XFab-α4-1BB/CD40L was generally well tolerated up to 510 nmol/kg dosed weekly for 5 weeks, as determined by clinical chemistry and histopathology results, suggesting that acceptable toxicity can be achieved at doses that induce immune effects.

Temporary increases in circulating T cells and decreases in B cells were noticed in animals with repeated XFab-α4-1BB/CD40L administration (Fig. 7a). Cytokine release was not observed in any of the groups until 24 h postdose, as IL-2, IL-10, IL-12, TNF-α, IFN-γ, and granzyme B levels were below lower limit of quantification. Therefore, the bispecific antibody showed acceptable pharmacodynamics and toxicity in NHPs with a single-dose and repeat-dose regimen that allowed T-cell activation.

Discussion

In this study, we demonstrate preclinical characterisation of a novel bispecific antibody, the XFab-α4-1BB/CD40L fusion protein, and corroborate the mechanism of action for potent tumour-specific immunity. The bispecific antibody manifests independent CD40 agonistic activity, similar to the physiological process where immature DCs are licensed by $CD40L^+$ CD4 T cells. Subsequently, the antibody helps to direct 4-1BB agonist activity to the area of DC maturation, thereby providing a focused costimulatory signal for specific

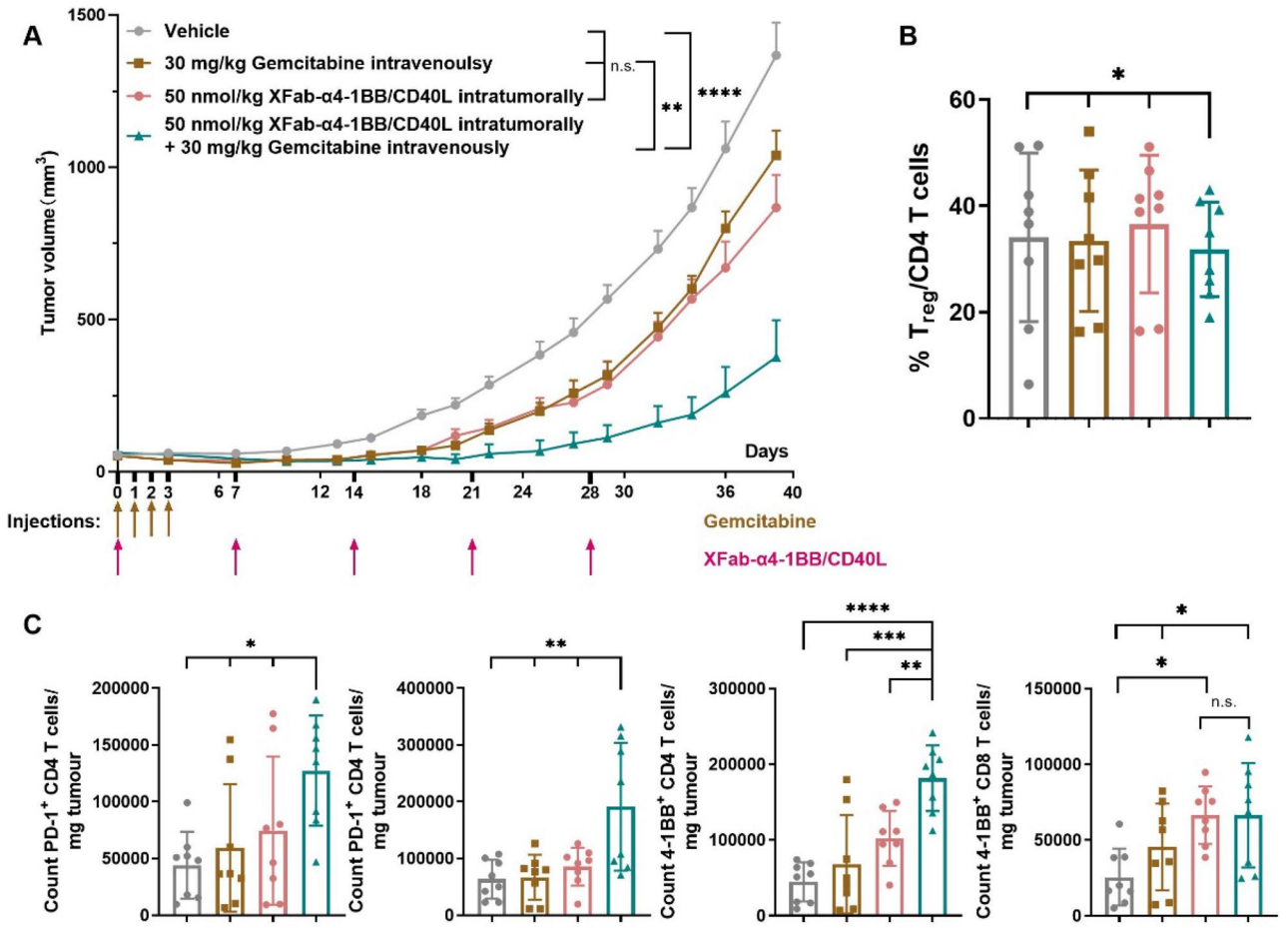

Fig. 6 Effect of XFab-α4-1BB/CD40L in combination with gemcitabine on the inhibition of tumour growth in Panc02 cell-bearing mice. **a** Human CD40×4-1BB transgenic mice were subcutaneously implanted with Panc02 cells at 5.0×10^6 per mouse. When tumours were approximately 50–90 mm^3, the mice were administered 30 mg/kg gemcitabine intravenously only or in combination with 50 nmol/kg XFab-α4-1BB/CD40L intratumourally at the indicated time points. Statistical analysis was performed by two-way repeated measure ANOVA with Tukey's multiple comparison test. **b** Digested tumour tissues at the end point were analysed by flow cytometry gating on T_{reg} and CD4 cells. **c** Tumour-infiltrating $CD4^+$ and $CD8^+$ T cells were analysed for 4-1BB and PD-1 expression by flow cytometry. Data points in (**b, c**) indicate mean ± SD ($n=6$–8 animals per group), and statistical significance was calculated using unpaired one-way ANOVA with Tukey's multiple comparison test

T-cell activation, proliferation, and effector function. Consistent with this mechanism of action, XFab-α4-1BB/CD40L demonstrates definite tumour growth inhibition in syngeneic tumour mouse models. Moreover, toxicology studies in non-human primates confirmed the safety profiles at the doses maintaining favourable immune activity.

CD40 and 4-1BB are two preclinically validated targets, which have manifested pharmacodynamic activity and certain clinical antitumour efficacy in monotherapy. However, for 4-1BB, liver inflammation is a key limiting factor and dose reduction is required for good-tolerance. A recent report confirmed the overall objective response rate for utomilumab (4-1BB mAb) was 3.8% in patients with solid tumours at the tolerated dose levels [23]. Another report demonstrated marginal clinical activity of utomilumab in immune checkpoint inhibitor-experienced melanoma and non-small cell lung cancer patient [24]. Similarly, a single-agent CD40 mAb has yielded minimal rates of objective tumour response. Selicrelumab, while producing objective partial responses in 27% of patients with advanced melanoma in the first-in-human study, showed a 0% objective overall response rate in a second trial [25]. For both targets, the current clinical strategy has shifted to combinatorial therapies. For example, CD40 agonists combined with anti-PD-1 antibodies have shown synergistic effects on the induction of T-cell immunity and antitumour responses in several preclinical tumour models, including immune-resistant tumours [26].

The use of 4-1BB and CD40 agonists is most likely feasible in combination regimen with no evidence of serious accumulative toxicity, and there is a rationale for the therapeutic synergy of this combined regimen. Specifically,

Table 1 Clinical observations after single and multiple doses of XFab-α4-1BB/CD40L in non-human primates

Single dose (n = 2)	Vehicle	765 nmol/kg
Liquid faeces	(0/2)	(0/2)
Sunken eyes and dry skin	(0/2)	(0/2)
Decreased activity	(0/2)	(0/2)
Reduced appetite	(0/2)	(0/2)

	Vehicle ($n = 10$)					20 nmol/kg ($n = 10$)					100 nmol/kg ($n = 10$)					510 nmol/kg ($n = 10$)				
	1st	2nd	3rd	4th	5th	1st	2nd	3rd	4th	5th	1st	2nd	3rd	4th	5th	1st	2nd	3rd	4th	5th
Liquid faeces	0	0	0	0	0	0	0	0	0	1	0	0	0	0	0	0	0	0	0	0
Sunken eyes and dry skin	0	0	0	0	0	0	0	0	0	1	0	0	0	0	0	0	0	0	0	0
Decreased activity	0	0	0	0	0	0	0	0	0	1	0	0	0	0	0	0	0	0	0	0
Reduced appetite	0	0	0	0	0	0	0	0	1	1	0	0	0	0	0	0	0	0	0	0
Weight loss	0	0	0	0	0	0	0	0	0	0	0	0	0	0	0	0	0	0	0	0
Elevated body temperature	1	0	0	0	0	0	0	0	0	2	0	0	0	0	0	0	0	0	0	2
Decreased body temperature	0	0	0	0	0	0	0	0	0	1	0	0	0	0	0	0	0	0	0	1
Abnormal ophthalmic findings	0	0	0	0	0	0	0	0	0	0	0	0	0	0	0	0	0	0	0	0

Non-human primates treated with a single or repeated intravenous dose were observed for clinical signs of adverse effects. In a single-dosing study, the maximal tolerated dose was at least 765 nmol/kg (upper). For the repeated dosing study, a male monkey receiving 20 nmol/kg repeated doses showed adverse effects including liquid faeces, sunken eyes and dry skin, decreased activity, reduced appetite, and decreased body temperature after the last administration (bottom). Supported care is needed afterwards. Slightly abnormal body temperature was observed in animals receiving repeated doses of 510 nmol/kg but returned to normal after 24 h

Table 2 Scoring of liver pathology after multiple doses of XFab-α4-1BB/CD40L in non-human primates

	Vehicle	20 nmol/kg	100 nmol/kg	510 nmol/kg
Degeneration with mixed inflammatory cells (parenchymal)				
Minimal	2	0	1	0
Mixed inflammatory cells in portal tracts				
Minimal	0	1	0	0
Degenerative hepatocyte				
Minimal	0	0	0	0

A scoring system was used to assess liver pathology in haematoxylin and eosin-stained sections according to hepatocellular necrosis, portal tract inflammation, and degenerative hepatocytes. The number of monkeys with minimal effect in each group are shown

conventional DC1 (cDC1) is paramount for 4-1BB agonists to induce antitumour efficacy in the role of cross-priming of CD8 T cells. On the other hand, CD40 agonists restore cDC1 abundance, promotes maturation [27] and improves the expansion of antigen-specific T cells [28]. Therefore, preclinical data have provided a clear justification for the simultaneous activation of CD40 and 4-1BB, making it a promising strategy to boost the priming and expansion of tumour-specific immunity.

Dendritic cells are central to the initiation of antigen-specific immunity; thus, manipulation of DCs holds great potential for inducing efficient antitumour immunity by conditioning the tumour microenvironment and mediating priming of antitumour T cells. In our study, XFab-α4-1BB/CD40L was confirmed to mature DCs in the absence of exogenous innate immune stimuli (Fig. 2). In this regard, the advantage of the bispecific antibody lies in directing 4-1BB agonist activity to the area of matured DC, thereby providing a focused stimulus for T-cell activation. Consequently, XFab-α4-1BB/CD40L-mediated crosslinking of DCs and T cells could provide tangible value in activation and amplification of antitumour responses based on T cells. This has been confirmed by the treatment of MC38 and MB49 tumours with XFab-α4-1BB/CD40L, which resulted in the proliferation and activation of intratumoural T cells, as shown by 4-1BB and PD-1 upregulation (Fig. 5). In addition, subpopulations of T cells including effector memory (EM) and central memory (CM) T cells were promoted, in line with earlier work related to CD40 and 4-1BB agonists [29].

The crux of treatment of tumours with low T-cell infiltration is inducing the priming of T cells. Activation of CD40 on DCs enhances tumour antigen cross-presentation

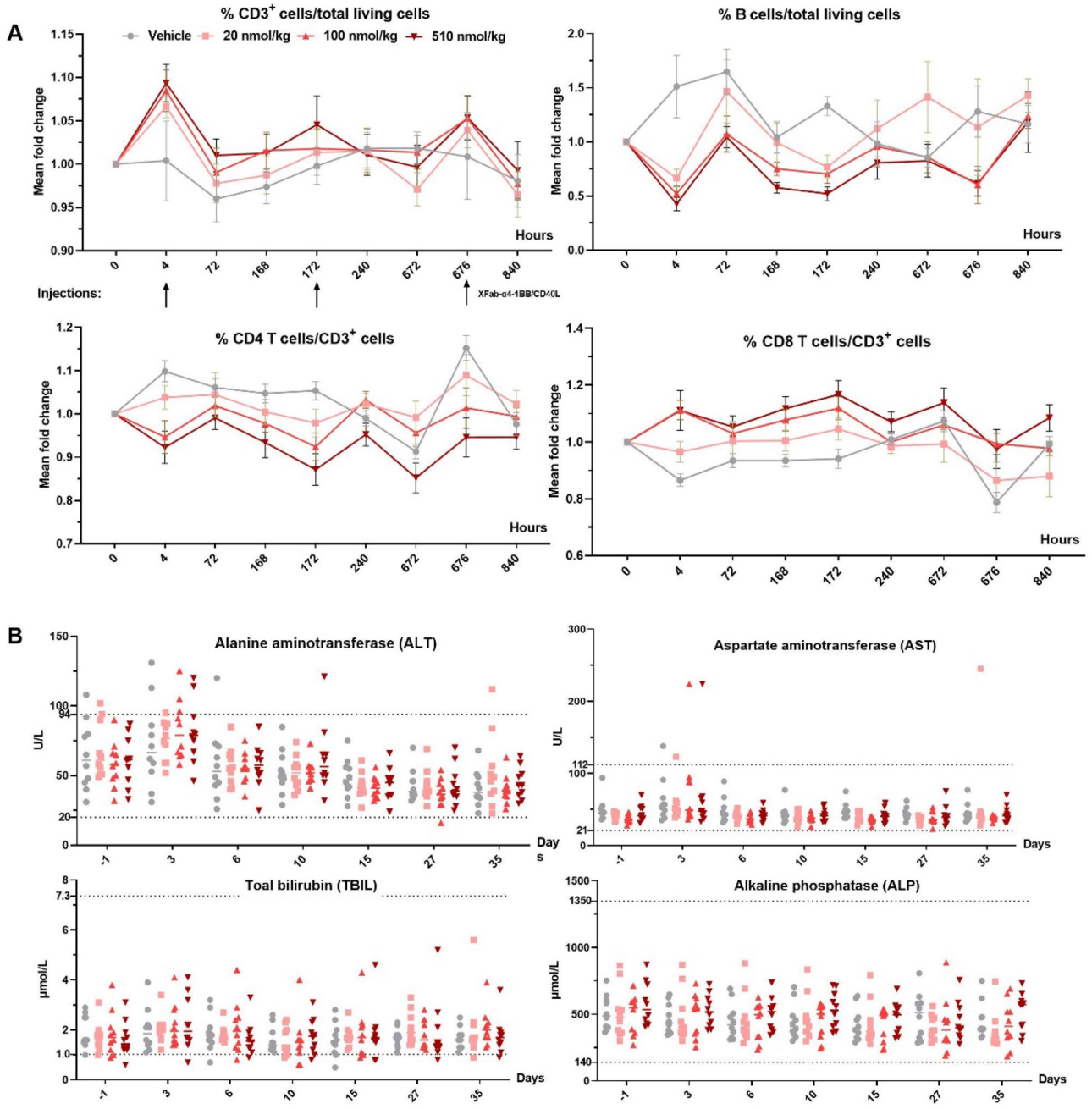

Fig. 7 Pharmacodynamic study and liver function documentation of repeat dosing of XFab-α4-1BB/CD40L in cynomolgus monkeys. Cynomolgus monkeys were treated with repeated doses of XFab-α4-1BB/CD40L at 20, 100, or 510 nmol/kg on days 0, 7, 14, 21, and 28. Blood samples were collected on the indicated time points and analysed for immune cell subsets by flow cytometry. **a** Kinetic changes in T cells and B cells ($CD20^+$). The mean fold change compared with predose ± SD was shown. **b** Kinetic changes in liver function. Dotted lines indicate normal range. $n = 10$ per group

and provides activation signals that mediate effective T-cell priming [30]. This process can be bolstered by increasing the availability of tumour antigens accessible for DC uptake through therapeutic cancer vaccines, chemotherapy and radiotherapy. Numerous preclinical studies have supported the critical role of CD40 activation in a vaccination setting for tumour regression [31, 32]. Our study depicts that in human transgenic mice immunised with ovalbumin protein, XFab-α4-1BB/CD40L reduced the growth of ovalbumin-expressing tumours as a prophylactic treatment. Moreover, in the Panc02-bearing mice, gemcitabine cooperates with XFab-α4-1BB/CD40L by spilling antigen, inducing more effective

DC cross-presentation and T-cell activation, accompanied by decreased regulatory T cells (Fig. 6). These data suggest that XFab-α4-1BB/CD40L holds the promise to act as an adjuvant and enhance antitumour efficacy of cancer vaccines as both prophylactic and therapeutic treatments.

An intratumoural route of administration may provide a feasible approach aiming to selectively direct CD40 and 4-1BB agonism to the tumour microenvironment. Earlier studies revealed that intratumoural treatment was able to induce abscopal effects characterised by systemic antitumour T-cell activity and a long-term memory response with lower toxicity [33]. In murine models with bladder cancer, local CD40 agonist administration led to accumulation in the tumour-draining lymph nodes and the spleen, most likely reflecting organs with $CD40^+$ immune cells, whereas systemic administration led to higher concentrations in the liver and blood [34]. In our study, greater tumour growth inhibition was observed in mice treated with local low-dose bispecific antibody (15 nmol/kg) compared with the even higher dose (5 nmol/kg) delivered intravenously (Fig. 5), implicating that systemic administration in this dose range results in a low concentration of antibody in the tumour or the lymph nodes, which is insufficient for T-cell activation. Several studies have confirmed that TILs naturally express high levels of 4-1BB and CD40 [19, 35]. Thus, an intratumoural route presents the advantage that agonist activity is directed to areas with increased expression of both targets, imparting abundant signals for XFab-α4-1BB/CD40L crosslinking.

An unwanted side effect of conventional bivalent binding molecules, such as IgGs, is the interaction with FcγIIB expressed by sinusoidal endothelial cells and macrophages in the liver. Liver toxicity was previously reported with 4-1BB agonist mAbs, including urelumab on a human IgG4 backbone and utomilumab on IgG1 backbone [36], whereas the bispecific antibody targeting 4-1BB/PD-L1 with no Fc-mediated effector function, proved to be safe from liver toxicity [5]. Beyond side effects, the antitumour efficacy dependent on intratumoural FcγIIB expression on tumour-associated myeloid cells and macrophages may arouse several concerns in that cells varied in FcγR levels across patients, making them a flimsy source of crosslinking-dependent activation [37]. To overcome these problems, we devised the bispecific antibody lack of Fc domain in nature based on the XFab® platform. The α4-1BB component was unable to induce 4-1BB signalling in the absence of CD40-mediated crosslinking, which is a significant safety feature of the protein. In cynomolgus monkeys, the bispecific antibody is well tolerated up to 51 mg/kg in a repeated regimen.

In a preclinical model, the combination therapy of CD40 and 4-1BB mAbs demonstrated a fourfold enhancement in the antigen-specific T-cell response compared with 4-1BB mAb alone [38]. These findings as well as the underpinning mechanism lay a solid foundation for the bispecific framework simultaneously targeting these two pathways. XFab-α4-1BB/CD40L acts as a bridge between CD40-expressing APCs and 4-1BB-expressing T cells, exerting superior activity for CD40 and 4-1BB signalling and therefore resulting in DC priming and T-cell effector functions.

In summary, we have developed an XFab-α4-1BB/CD40L fusion protein, a bispecific antibody with a novel mode of action and potentially improved efficacy for the treatment of cancers. The XFab-α4-1BB/CD40L fusion protein was developed by Immunoah for the treatment of solid tumours. The results presented herein illustrate that XFab-α4-1BB/CD40L potently activates DCs and improves the priming and expansion of antigen-specific T cells, which subsequently leads to tumour growth inhibition in vivo. Our data also support the notion that XFab-α4-1BB/CD40L is a promising tool that acts as an adjuvant and enhances the antitumour efficacy of cancer vaccines as both prophylactic and therapeutic treatments.

Materials and methods

Preparation of XFab-α4-1BB/CD40L and control therapeutic agents

The XFab-α4-1BB/CD40L fusion protein (IMB071703) was designed based on the XFab® platform (patent no. CN110669137B), using the following polypeptide chains: (1) a VL from sytalizumab (patent no. CN108367075A) fused to κ chain followed by two ectodomains of CD40L (from UniProtKB P29965) and (2) a VH from sytalizumab fused to CH1 from IgG1 followed by one ectodomain of CD40L. Vectors of XFab-α4-1BB/CD40L were constructed using recombinant DNA technology, and the constructed vectors were stably expressed in CHO cells using a Gene Pulser Xcell™ Electroporation Systems (Bio-Rad, USA) at 37 °C for 20 days in a CO_2 incubator equipped with a rotating shaker. Besides, the anti-4-1BB mAb, viz. sytalizumab, and CD40L-Fc were used as control therapeutic agents. Sytalizumab was a bivalent anti-4-1BB mAb in a human IgG4 backbone developed by Immunoah. CD40L-Fc consisted of two ectodomains of CD40L, each of which was connected by an Fc domain from human IgG4.

Cell lines

If not indicated differently, all cell media and supplements were obtained from Gibco by Life Technologies. HEK293T-hu4-1BB cells were purchased from Genomeditech (#GM-C05172) and HEK-Blue CD40L cells from InvivoGen (hkb-cd40). HEK293T cells were obtained from KYinno

Biotechnology (Beijing, China). The signalling reporter cell line HEK-Blue CD40L was originally purchased from InvivoGen. HEK-Blue 4-1BB was generated by transfection of HEK-Blue CD40L cells with hu4-1BB-encoding plasmid DNA and cultured under 200 ug/mL hygromycin B (InvivoGen, 10687010). HEK293T-huCD40 was generated by transfection of HEK293T cells with huCD40-encoding plasmid DNA and cultured under 200 ug/mL hygromycin B (InvivoGen, 10687010).

B16-OVA MO4 mouse melanoma cell line (Sigma-Aldrich, SCC420) was cultured in complete RPMI-1640 (Corning, 10-040-CV) supplemented with 10% (v/v) foetal bovine serum. Mouse colon adenocarcinoma cell line MC38 (Kerafast, ENH204-FP) was cultured in complete DMEM (Corning, 23-10-013-CV) supplemented with 10% (v/v) foetal bovine serum (GeminiBio, 900-108). Mouse bladder carcinoma cell line MB49 was cultured in RPMI-1640 with 10% foetal bovine serum. Mouse pancreatic ductal adenocarcinoma cell line Panc02 which was purchased from National Infrastructure of Cell Line Resource, was cultured in complete DMEM supplemented with 5% (v/v) foetal bovine serum. Cell lines were analysed for authenticity using the respective cell bank (using DNA fingerprinting techniques, such as short tandem repeat profiling). All cell lines were tested for mycoplasma using MycoBlue Mycoplasma Detector (Vazyme, China) and shown to be mycoplasma-free.

Biolayer interferometry (BLI)

Target binding affinity of the bispecific antibody was measured using biolayer interferometry on an Octet QK system (ForteBio). Ni–NTA biosensors were loaded with recombinant human CD40 ECD fused to a His-tag (CD40-His, 10 μg/mL; Sino Biological, 10774-H08H) or recombinant human 4-1BB ECD fused to a His-tag (4-1BB-His, 10 μg/mL; Immunoah, 20210528) diluted in PBS. After a baseline measurement in PBS, a dilution series of the bispecific antibody was injected for association and the dissociation phase monitored for 180 and 300 s, respectively. Data were acquired using Data Acquisition Software (ForteBio, v9.9.9.49d) and analysed with Data Analysis Software (ForteBio, v9.0.0.14). Data were fitted with the 1:1 Global Full fit model.

T-cell isolation

Peripheral blood mononuclear cells (PBMCs) were isolated from buffy coats of healthy human blood donors (Beijing Immunoah Pharma Tech Co., Ltd.) by density centrifugation over a Ficoll–Paque gradient (Ficoll-Paque PLUS medium, VWR, 17-5446-02). T cells were enriched from PBMCs by immunomagnetic negative selection, using EasySep Human T-Cell Isolation Kit (STEMCELL, 17951) and EasySep Magnet (STEMCELL, 18000).

Cell-based binding assays

For the binding assays, HEK293-hu4-1BB cells (Genomeditech, GM-C05172) or HEK-Blue CD40L cells (InvivoGen, hkb-cd40) were incubated with titrated concentrations of XFab-α4-1BB/CD40L for 30 min at 4 ℃. The cells were washed and incubated for 30 min at 4 ℃ in FACS buffer containing 10 mL/test APC-conjugated anti-human Ig light chain kappa antibody (BioLegend, 392708) before being washed and resuspended in FACS buffer. HEK293T-hu4-1BB and HEK293T-cy4-1BB were generated by transfection of HEK293T cells with hu4-1BB or cy4-1BB-encoding plasmid DNA and cultured under 200 μg/mL hygromycin B (InvivoGen, 10687010). If binding on B cells or 4-1BB-expressing HEK293 T cells was performed, human, mouse, or cynomolgus whole blood was incubated with biotin-conjugated XFab-α4-1BB/CD40L followed by in-house red blood cell lysis buffer. After washing, cells were incubated with 10 ml/test PE-conjugated anti-streptavidin antibody (BioLegend, 410504) for 30 min at 4 ℃. Additional flow cytometry detection antibodies for human CD20 or mouse CD19 were added to allow gating on B cells.

Agonist activity assays

CD40 agonist activity was evaluated using HEK-Blue CD40L reporter cells (InvivoGen, San Diego, CA, USA), which served to measure the bioactivity of CD40L through the secretion of embryonic alkaline phosphatase (SEAP) upon NF-κB activation following CD40 stimulation. HEK-Blue CD40L cells were cocultured with titrated concentrations of XFab-α4-1BB/CD40L fusion protein. 4-1BB agonist activity was evaluated using HEK-Blue-hu4-1BB cells, cocultured with or without HEK293T-huCD40 in the presence of XFab-α4-1BB/CD40L. SEAP was subsequently quantified with QUANTI-Blue Solution (InvivoGen, rep-qbs2) by measuring the optical density at 620 nm using a CLARIOstar Plus instrument (BMG LABTECH, Ortenberg, Hessen, Germany).

Maturation of dendritic cells

Monocyte-derived dendritic cells (All Cells, PB-DC001F-C) were incubated with dilution series of XFab-α4-1BB/CD40L or cytokines (4000 U/mL IL-6 (Peprotech, 200-06), 40 ng/mL IL-1β (Peprotech, 200-01B) and 40 ng/mL TNF-α (Peprotech, 300-01A) in serum-free DC medium (Nobimpex, 0295Z) for 48 h. Upregulation of the maturation markers CD86 and HLA-DR was analysed by flow

cytometry. Secretion of IL12p40 was measured by human IL12p40 ELISA kit (MULTISCIENCES, EK1183).

Mix-lymphocyte reaction (MLR) assays

For MLR assays, monocyte-derived dendritic cells were cultured in serum-free DC medium supplemented with 1000 U/mL GM-CSF (Peprotech, 300-03) and 500 U/mL IL-4 (Peprotech, 200-04) in suspension culture flasks. Fresh GM-CSF and IL-4 were supplied as appropriate. After 5 days, 2 mg/mL ovalbumin (OVA; Sigma-Aldrich, A5503) was added and incubated for 4 h. OVA-loaded DCs were then incubated in serum-free DC medium supplemented with 4000 U/mL IL-6, 40 ng/mL IL-1β and 40 ng/mL TNF-α for 48 h to obtain mature DCs prior to MLR assays. T cells (2×10^5 cells/well) labelled with CellTrace Violet Cell Proliferation Kits (ThermoFisher, C34571) were cocultured with OVA-loaded mature DCs (1×10^5 cells per well) in the presence of titrated bispecific antibodies or control antibodies in a 96-well culture plate for 10 days. T-cell proliferation and activation were analysed by flow cytometry. Confocal images were captured on a 24-well imaging plate (Cellvis, P24-1.5H-N) using a Nikon AX confocal laser microscope (Nikon, Tokyo, Japan).

Expansion of antigen-specific T cells in a vaccination mouse model

Immunocompetent human 4-1BB/CD40 transgenic mice (C57BL/6-*Tnfrsf9*$^{tm1(TNFRSF9)}$*Cd40*$^{tm1(CD40)}$/Bcgen) were purchased from (Biocytogen, Beijing). The expansion of ovalbumin (OVA)-specific T cells was studied in OVA vaccination models. The mice were immunised with 12.5 mg/kg OVA (Sigma-Aldrich, A5503) or vehicle intradermally on 7 occasions. Additionally, the mice were administered indicated doses of XFab-α4-1BB/CD40L or 1.25 mg/kg poly (I:C) (Sigma-Aldrich, P1530) intradermally on the same day. Whole blood samples were collected for flow cytometry. On day 24, mice were subcutaneously inoculated with 5×10^5 B16-OVA cells in the right flank. Tumour growth was continuously measured by calliper measurement (tumour volume $[mm^3]=0.5\times[length]\times[width]^2$. Tumour single-cell suspensions were analysed by flow cytometry on day 50.

In vivo antitumoural effect

Six to eight-week-old human 4-1BB/CD40 transgenic mice were implanted subcutaneously into the flank with MC38 or MB49 cells at 2.0×10^5 cells per mouse on study day 0. When tumours were approximately 50–90 mm^3, the mice were administered vehicle (PBS) or XFab-α4-1BB/CD40L. For the combination therapy experiment, 2.0×10^6 Panc02 cells were inoculated, and the mice were treated with gemcitabine alone or in combination with XFab-α4-1BB/CD40L. Tumour growth was monitored three times per week. At the end of the experiment, flow cytometry was used to determine the number of T-cell subsets.

Flow cytometry staining

Dead cells were stained in all experiments using the Zombie Aqua Fixable Viability Kit (423101, BioLegend) for differentiation. Cell surface markers were stained with specific antibodies for 30 min at 4 ℃ in the dark. Intracellular markers were stained using antibodies for 45 min at 4 ℃ after the cells were fixed and permeabilised using a permeabilisation buffer (421002, BioLegend). Data were acquired using a NovoCyte Flow Cytometer System (Agilent, Santa Clara, CA, USA) and analysed using NovoExpress software.

Antibodies listed for cell-marker staining were purchased from BioLegend: anti-mouse CD3 FITC (100204), anti-mouse CD4 APC/Cy7 (100414), anti-mouse CD8 BV510 (102042), anti-mouse CD44 PE/Cy7 (103030), anti-mouse CD45 PerCP/Cy5.5 (103132), anti-mouse CD62L BV421 (104436), anti-mouse CD279 APC (109112), anti-human CD137 PE/Cy5 (309804), anti-human CD20 APC (302310), anti-human CD86 (305412), anti-human HLA-DR PE (327008), anti-human CD3 FITC (300406), anti-human CD4 APC/Cy7 (357416), anti-human CD8 APC (301014), and anti-human CD25 PE/Cy7 (302612). Other antibodies include H-2 Kb OVA Tetramer-SIINFEKL (TS-5001-1C, MBL International), anti-mouse CD8 FITC (D271-4, MBL International anti-mouse), and anti-human Foxp3 PE (320008, Invitrogen).

In vitro cytokine release assay

PBMCs (1×10^5 cells/well) were incubated with the indicated concentrations of bispecific antibody in 96-well cell culture plates for 24 h at 37 ℃. Cytokines in the supernatants were measured using Human XL Cytokine Luminex® Performance Panel Premixed Kit (R&D Systems, FCSTM18B) on a Luminex 200 System.

Toxicity and immune stimulation in non-human primates (NHPs)

Immunophenotyping of peripheral blood was performed to assess peripheral lymphocyte subpopulations by flow cytometry. Plasma samples were analysed for cytokines using NHP XL Cytokine Luminex® Performance Panel Premixed Kit (R&D Systems, FCSTM21) on a Luminex 200 System.

For toxicology study, single-dosing groups of vehicle or 765 nmol/kg intravenous infusions were presented (2/group). The repeat-dosing groups consists of animals (10/group) receiving five infusions of XFab-α4-1BB/CD40L

on days 0, 7, 14, 21, and 28. The study was terminated 35 days after the first administration of repeat-dose animals and 15 days after the administration of single-dose animals.

Liver toxicity assessment was conducted for the repeat-dose animals, where liver samples were taken at necropsy for histological assessment on day 35. Liver samples were sectioned and subjected to histopathological evaluation via haematoxylin and eosin staining. Liver sections were scored by a certified pathologist for pathology.

Statistical analysis

GraphPad Prism 9.00 was used for statistical analysis. EC_{50} values were determined using nonlinear regression curve, fit variable slope (four parameters), and least-squares fit. Data are shown as mean with SD or SEM. The statistical tests used are indicated in the figure legends for each experiment. *P* values are indicated by asterisks as * < 0.05, ** < 0.01, ***0.001, ****0.0001.

Supplementary Information The online version contains supplementary material available at https://doi.org/10.1007/s00262-023-03535-y.

Acknowledgements The authors would like to thank all their colleagues at Beijing Immunoah Pharma Tech Co. Ltd. for providing useful suggestions for experimental design, animal husbandry, and technical assistance.

Author contributions BW and YL were involved in investigation, conception and design, validation of methodology, data analysis and interpretation, visualisation, and writing and revision of the manuscript. RY, XD, GX, NQ, and XP were involved in investigation, conception and design, and validation of methodology. QX was involved in pathology assessment and technical support. BD, CY, HL, JW, and GB were involved in technical and material support. LL was involved in administrative and material support and review of the manuscript. XG was involved in investigation, conception and design, development of methodology, analysis and interpretation of data, review of the manuscript, and study supervision.

Funding This research received no external funding.

Data availability All the data generated in this study are available upon reasonable request from the corresponding author.

Declarations

Conflict of interest The authors have no relevant financial or non-financial interests to disclose.

Ethics approval All animal experiments were performed under the American Veterinary Medical Association (AVMA) Guidelines for the Euthanasia of Animals (2020 Edition) and the Laboratory Animal Guidelines for euthanasia of China, approved by the Committee of Animal Experiments and Experimental Animal Welfare of Beijing Immunoah Pharma Tech Co., Ltd. (approval number: IACUC2021-0096) and were in strict accordance with the 3R principles (reduction, replacement, and refinement).

References

1. Waldman AD, Fritz JM, Lenardo MJ (2020) A guide to cancer immunotherapy from T-cell basic science to clinical practice. Nat Rev Immunol 20:651–668
2. Chen DS, Mellman I (2017) Elements of cancer immunity and the cancer-immune set point. Nature 541:321–330
3. Chester C, Sanmamed MF, Wang J, Melero I (2018) Immunotherapy targeting 4-1BB mechanistic rationale clinical results and future strategies. Blood 131:49–57
4. Betof Warner A, Palmer JS, Shoushtari AN et al (2020) Long-term outcomes and responses to retreatment in patients with melanoma treated with PD-1 blockade. J Clin Oncol Off J Am Soc Clin Oncol 38:1655–1663
5. Lakins MA, Koers A, Giambalvo R et al (2020) FS222 a CD137/PD-L1 tetravalent bispecific antibody exhibits low toxicity and antitumor activity in colorectal cancer models. Clin Cancer Res Off J Am Assoc Cancer Res 26:4154–4167
6. Bartkowiak T, Curran MA (2015) 4-1BB agonists multi-potent potentiators of tumor immunity. Front Oncol 5:117
7. Shuford WW, Klussman K, Tritchler DD et al (1997) 4-1BB costimulatory signals preferentially induce CD8+ T-cell proliferation and lead to the amplification in vivo of cytotoxic T-cell responses. J Exp Med 186:47–55
8. Saoulli K, Lee SY, Cannons JL et al (1998) CD28-independent, TRAF2-dependent costimulation of resting T-cells by 4-1BB ligand. J Exp Med 187:1849–1862
9. Wilcox RA, Tamada K, Flies DB et al (2004) Ligation of CD137 receptor prevents and reverses established anergy of CD8+ cytolytic T lymphocytes in vivo. Blood 103:177–184
10. Hernandez-Chacon JA, Li Y, Wu RC et al (2011) Costimulation through the CD137/4-1BB pathway protects human melanoma tumor-infiltrating lymphocytes from activation-induced cell death and enhances antitumor effector function. J Immunother 34:236–250
11. Kawalekar OU, O'Connor RS, Fraietta JA et al (2016) Distinct signaling of coreceptors regulates specific metabolism pathways and impacts memory development in car T-cells. Immunity 44:380–390
12. Gao J, Wang Z, Jiang W et al (2023) CLDN18.2 and 4-1BB bispecific antibody givastomig exerts antitumor activity through CLDN18.2-expressing tumor-directed T-cell activation. J Immunother Cancer 11:e006704
13. Muik A, Adams HC 3rd, Gieseke F et al (2022) DuoBody-CD40x4-1BB induces dendritic-cell maturation and enhances T-cell activation through conditional CD40 and 4-1BB agonist activity. J Immunother Cancer 10:e004322
14. Melero I, Tanos T, Bustamante M et al (2023) A first-in-human study of the fibroblast activation protein-targeted 4-1BB agonist RO7122290 in patients with advanced solid tumors. Sci Transl Med 15:eabp9229
15. Cheng LS, Zhu M, Gao Y et al (2023) An Fc-muted bispecific antibody targeting PD-L1 and 4-1BB induces antitumor immune activity in colorectal cancer without systemic toxicity. Cell Mol Biol Lett 28:47
16. Muik A, Altintas I, Gieseke F et al (2022) An Fc-inert PD-L1×4-1BB bispecific antibody mediates potent anti-tumor immunity in mice by combining checkpoint inhibition and conditional 4-1BB co-stimulation. Oncoimmunology 11:2030135
17. Cendrowicz E, Jacob L, Greenwald S et al (2022) DSP107 combines inhibition of CD47/SIRPα axis with activation of 4-1BB to trigger anticancer immunity. J Exp Clin Cancer Res CR 41:97
18. Snell D, Gunde T, Warmuth S et al (2023) An engineered T-cell engager with selectivity for high mesothelin-expressing cells

and activity in the presence of soluble mesothelin. Oncoimmunology 12:2233401
19. Ye Q, Song DG, Poussin M et al (2014) CD137 accurately identifies and enriches for naturally occurring tumor-reactive T-cells in tumor. Clin Cancer Res Off J Am Assoc Cancer Res 20:44–55
20. Gros A, Robbins PF, Yao X et al (2014) PD-1 identifies the patient-specific $CD8^+$ tumor-reactive repertoire infiltrating human tumors. J Clin Investig 124:2246–2259
21. Vonderheide RH (2018) The immune revolution: a case for priming Not Checkpoint. Cancer Cell 33:563–569
22. Hünig T (2016) The rise and fall of the CD28 superagonist TGN1412 and its return as TAB08: a personal account. FEBS J 283:3325–3334
23. Segal NH, He AR, Doi T et al (2018) Phase I study of single-agent utomilumab (PF-05082566), a 4-1BB/CD137 agonist in patients with advanced cancer. Clin Cancer Res Off J Am Assoc Cancer Res 24:1816
24. Hong DS, Gopal AK, Shoushtari AN et al (2022) Utomilumab in patients with immune checkpoint inhibitor-refractory melanoma and non-small-cell lung cancer. Front Immunol 13:897991
25. Vonderheide RH (2020) CD40 agonist antibodies in cancer immunotherapy. Annu Rev Med 71:47–58
26. Irenaeus SMM, Nielsen D, Ellmark P et al (2019) First-in-human study with intratumoral administration of a CD40 agonistic antibody ADC-1013 in advanced solid malignancies. Int J Cancer 145:1189–1199
27. Lin JH, Huffman AP, Wattenberg MM et al (2020) Type 1 conventional dendritic cells are systemically dysregulated early in pancreatic carcinogenesis. J Exp Med 217:e20190673
28. Deronic A, Nilsson A, Thagesson M, Werchau D, Enell Smith K, Ellmark P (2021) The human anti-CD40 agonist antibody mitazalimab (ADC-1013; JNJ-64457107) activates antigen-presenting cells, improves expansion of antigen-specific T-cells and enhances anti-tumor efficacy of a model cancer vaccine in vivo. Cancer Immunol Immunother 70:3629–3642
29. Claus C, Ferrara C, Xu W et al (2019) Tumor-targeted 4-1BB agonists for combination with T-cell bispecific antibodies as off-the-shelf therapy. Sci Transl Med 11:eaav5989
30. Yin W, Gorvel L, Zurawski S et al (2016) Functional specialty of CD40 and dendritic cell surface lectins for exogenous antigen presentation to CD8(+) and CD4(+) T-cells. EBioMedicine 5:46–58
31. Lau SP, van Montfoort N, Kinderman P et al (2020) Dendritic cell vaccination and CD40-agonist combination therapy licenses T-cell-dependent antitumor immunity in a pancreatic carcinoma murine model. J immunother cancer 8:e000772
32. Nimanong S, Ostroumov D, Wingerath J et al (2017) CD40 signaling drives potent cellular immune responses in heterologous cancer vaccinations. Cancer Res 77:1918–1926
33. Knorr DA, Dahan R, Ravetch JV (2018) Toxicity of an Fc-engineered anti-CD40 antibody is abrogated by intratumoral injection and results in durable antitumor immunity. Proc Natl Acad Sci USA 115:11048–11053
34. Sandin LC, Orlova A, Gustafsson E et al (2014) Locally delivered cd40 agonist antibody accumulates in secondary lymphoid organs and eradicates experimental disseminated bladder cancer. Cancer Immunol Res 2:80–90
35. Ishikawa K, Miyamoto M, Yoshioka T et al (2008) Up-regulation of CD40 with juxtacrine activity in human nonsmall lung cancer cells correlates with poor prognosis. Cancer 113:530–541
36. Melero I, Sanmamed MF, Glez-Vaz J, Luri-Rey C, Wang J, Chen L (2022) CD137 (4-1BB)-based cancer immunotherapy on its 25th anniversary. Cancer Discov 13(3):OF1–OF19
37. Stewart R, Hammond SA, Oberst M, Wilkinson RW (2014) The role of Fc gamma receptors in the activity of immunomodulatory antibodies for cancer. J Immunother Cancer 2:29
38. Gray JC, French RR, James S, Al-Shamkhani A, Johnson PW, Glennie MJ (2008) Optimising anti-tumour CD8 T-cell responses using combinations of immunomodulatory antibodies. Eur J Immunol 38:2499–2511